

High-Resolution Electron-Microscopy Study and Structure Modeling of the Stable Decagonal Al-Cu-Co Quasicrystal

H. Chen,⁽¹⁾ S. E. Burkov,^{(2),(a)} Y. He,⁽²⁾ S. J. Poon,⁽²⁾ and G. J. Shiflet⁽¹⁾

⁽¹⁾Department of Materials Science, University of Virginia, Charlottesville, Virginia 22901

⁽²⁾Department of Physics, University of Virginia, Charlottesville, Virginia 22901

(Received 5 April 1990)

We report the observation of a spatial quasiperiodicity in high-resolution electron-microscope images of the thermodynamically stable decagonal Al₆₅Cu₁₅Co₂₀ quasicrystal. Well defined quasiperiods consistent with decagonal symmetry and x-ray-diffraction data have been found. The structure observed is inconsistent with conventional ideal Penrose tiling. There is strong evidence for an entropy stabilization mechanism.

PACS numbers: 61.16.Di, 61.42.+h, 68.65.+g

The recently discovered stable Al₆₅Cu₁₅Co₂₀ decagonal quasicrystal¹ provides a unique opportunity for an experimental study of two-dimensional quasiperiodicity. Unlike previously obtained² metastable decagonal quasicrystals this alloy exhibits extremely sharp diffraction peaks (correlation length³ is about 2000 Å); and they can be made by both rapid quenching and conventional casting.¹ In fact, faceted single grains of this material, a few mm in size, have been grown and characterized.^{1,3} These are convincing evidences that Al₆₅Cu₁₅Co₂₀ is a stable decagonal quasicrystal. To date, there exist different structure models for quasicrystalline materials, and these models can be divided into two groups. In the first group,⁴⁻⁸ a decagonal quasicrystal is described by an ideal Penrose tiling.⁹ Structure models from the second group¹⁰⁻¹³ are based on entropic arguments and do not predict ideal quasiperiodicity but only "average" quasiperiodicity, with strong thermal phason fluctuations. Recently, Kortan *et al.* used scanning tunneling microscopy (STM) to study the decagonal Al₆₅Cu₁₅Co₂₀ quasicrystal.¹⁴ Their analysis based on a small region of the STM images led to a tiling model. In this work, however, close examination of the high-resolution electron-microscope (HREM) images of Al₆₅Cu₁₅Co₂₀ reveals that this particular stable phase cannot be described by an ideal Penrose tiling. Also, there is strong evidence that the stability of this decagonal phase is entropic in origin.

An alloy ingot of Al₆₅Cu₁₅Co₂₀ was made by melting nominal amounts of high-purity elements in an arc furnace under an argon atmosphere. The rapidly solidified ribbon samples were produced by melt spinning. The ribbons were sealed under vacuum in a quartz tube and annealed at 900°C for 24 h to reduce the possible phason strain. These samples were thinned for HREM studies by ion milling. Thin-film samples were prepared by sputtering from an Al₆₅Cu₁₅Co₂₀ target in an rf magnetron sputtering system on glass and NaCl substrates at 400°C. Thin films for HREM studies were obtained by dissolving the NaCl substrate in pure water. They were

further thinned by ion milling. Samples prepared by both techniques were checked by x-ray diffraction and conventional TEM, and both possessed decagonal quasicrystalline diffraction patterns.¹ A JEOL-4000EX transmission electron microscope was used to study the atomic images of both ribbon and thin-film samples. Special care has been taken to avoid the quasicrystalline-to-crystalline transformation induced by electron-beam irradiation.¹⁵

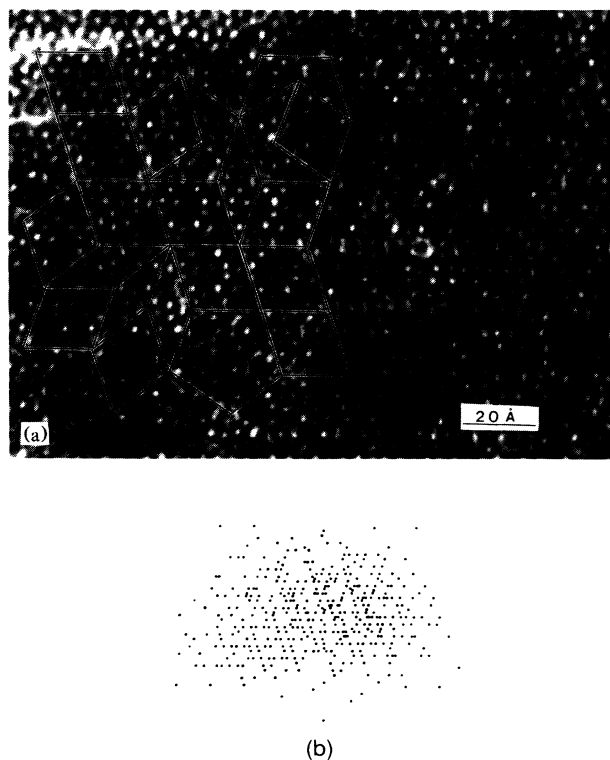


FIG. 1. (a) A portion of HREM image of a decagonal Al₆₅Cu₁₅Co₂₀ quasicrystal. The sample was prepared by melt quenching, and was further annealed at 900°C for 24 h. (b) Projection of the ring centers onto the perpendicular space.

Analysis of the HREM images is based on the basic property of a quasiperiodic pattern, namely, that any finite fragment of the whole pattern is repeated in space, but not periodically. This approach is slightly different from the usual practice.^{1,14,15} Previously, experimentalists tried to find tiles which were extensively used by theoreticians in their attempts to describe quasicrystals. Here, a more general definition of quasiperiodicity was used, which includes a quasiperiodic tiling as a particular case. The most recognizable fragment was chosen in the analysis, which is a ring about 20 Å in diameter with ten bright spots situated symmetrically [Figs. 1(a) and 2(a)]. These can also be found in the STM images.¹⁴ In fact, locally, the arrangement of these rings in our HREM images is quite similar to that in the STM images. Even though the details as small as 2 Å can be distinguished in the micrograph, the inflated tiles with tile sides of about 20 Å [Fig. 1(a)] were chosen in order to minimize misjudgement in the analysis. Centers of the rings were marked and their positions in plane were examined. Coordinates of all the ring centers [Fig. 1(a)] can be written in the following form:

$$\mathbf{X} = \sum_{j=1}^5 N_j \mathbf{A}_j, \quad (1)$$

where N_j are integers and \mathbf{A}_j are of 20-Å length and

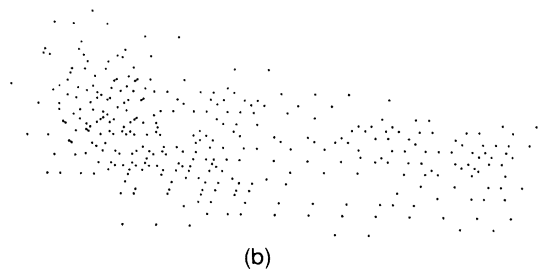
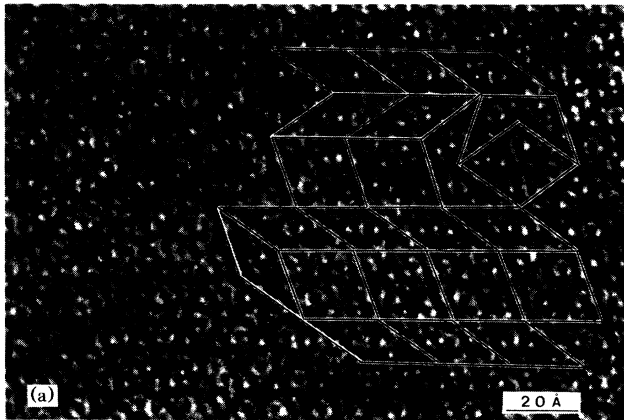


FIG. 2. HREM image of a $\text{Al}_{65}\text{Cu}_{15}\text{Co}_{20}$ sample made by sputter deposition at 400°C, without further annealing. (b) Projection onto the perpendicular space.

form a regular five star. The smallest spatial scale (in the case of an ideal Penrose tiling it would be a tile side) deduced from the (10000) peak in the x-ray-diffraction spectrum³ is 4 Å. The length of the \mathbf{A} vectors in Figs. 1(a) and 2(a) is related to the above length $a \approx 4$ Å by a simple inflation relation:

$$A = 2\tau^2 a \cos 18^\circ, \quad (2)$$

where $\tau = 1.618\dots$ is a golden mean. Therefore, the \mathbf{A}_j 's are some fundamental quasiperiods. Connecting the ring centers by the \mathbf{A} vectors throughout the micrograph can be accomplished by the three tiles: two Penrose rhombi and a crown (a regular pentagon can be decomposed into a fat rhombus and a crown). In fact, one can further decompose these two Penrose rhombi and crown into two isosceles triangles with sides as $A, A, A/\tau$, and $A/\tau, A/\tau, A$, respectively. In this manner, the whole micrograph can also be covered by these two types of triangles.¹⁵

A number of micrographs made from different samples, both as quenched ribbon annealed at 900°C for 24 h and thin film made by deposition at 400°C without annealing, were examined in this fashion. The largest micrograph of the annealed samples contains about 400 rings, a part of it is shown in Fig. 1(a). There are some regions where rings are not clearly seen; however, all these empty spaces can be covered by the tiles, though not unambiguously. That is, there are no unfillable regions. These empty regions may be due to sample-thickness variation or other conditions affecting the quality of an HREM image.

Is the tiling, obtained from the HREM image of annealed $\text{Al}_{65}\text{Cu}_{15}\text{Co}_{20}$ [Fig. 1(a)], consistent with an ideal Penrose tiling? To answer this question it suffices to inspect the ideal Penrose tiling [Fig. 3(a)]. The rings with ten symmetrically situated spots might be associated with stars of the Penrose tiling. Connecting centers results in a new tiling. The side of a large tile is related to the side of an original tile by Eq. (2) as well. But the tiling itself is just an inflated Penrose tiling, consisting of only two rhombi. There are no crowns nor pentagons. Thus, the experimental image is inconsistent with an ideal Penrose tiling.

However, even with a conventional Penrose tiling there are different generalizations and modifications of it. To check whether they are consistent with the experimental data, it is useful to lift the experimentally obtained tiling up to the 5D space; thus, one can express the coordinates of the centers of all the rings in Fig. 1(a) in terms of the 5D integer points $(N_1, N_2, N_3, N_4, N_5)$. Then, project the obtained array of 5D points onto the space perpendicular to the strip of ideal Penrose tiling.^{8,11,12} The above-defined mapping is not a one-to-one mapping. Since the sum of all five \mathbf{A}_j is zero, the simultaneous increment of all N_j by 1 changes a 5D integer vector but leaves a ring's center unaltered. To make the mapping unambiguous, all 5D integer points which differ by the (1,1,1,

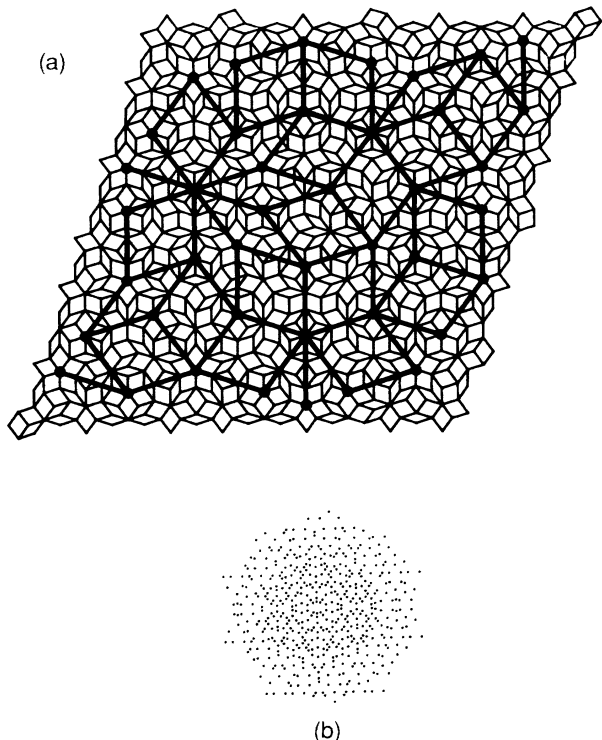


FIG. 3. (a) Ideal Penrose tiling and its inflation. (b) Projection onto the perpendicular space.

1,1) vector only must be identified. This identification effectively reduces the dimensionality of the perpendicular space from 3 to 2, merging the points with different coordinates in the (1,1,1,1,1) direction. The projection of the points derived from a HREM image is shown in Fig. 1(b). It clearly does not resemble a decagonally symmetric cloud expected for a Penrose tiling [Fig. 3(b)]. It is also important to calculate an average size of the perpendicular projection,

$$\langle X_{\perp}^2 \rangle = \frac{1}{N} \sum \left(X_{\perp i} - \frac{1}{N} \sum X_{\perp i} \right)^2, \quad (3)$$

as a function of the number of points N . For both an ideal Penrose tiling and all its modifications this value remains confined as N increases. The random-tiling theories¹⁰⁻¹³ predict a logarithmic divergence of this quantity: $\langle X_{\perp}^2 \rangle = (2\pi K)^{-1} \ln N$, where K is a phason stiffness. Experimental results are presented in Fig. 4. A limited number of points and experimental uncertainties may not permit the conclusion that the plot is strictly logarithmic. However, there is a "logarithmiclike" increase of $\langle X_{\perp}^2 \rangle$, in apparent agreement with both the random-tiling model¹⁰⁻¹³ and a model of an energetically stabilized quasicrystal with well developed thermal phason fluctuation.¹⁶ These results rule out any possible generalization of a Penrose tiling and cast a doubt on both matching-rule theories⁷ and the growth mechanisms⁶ which lead to an ideal Penrose tiling. The phason

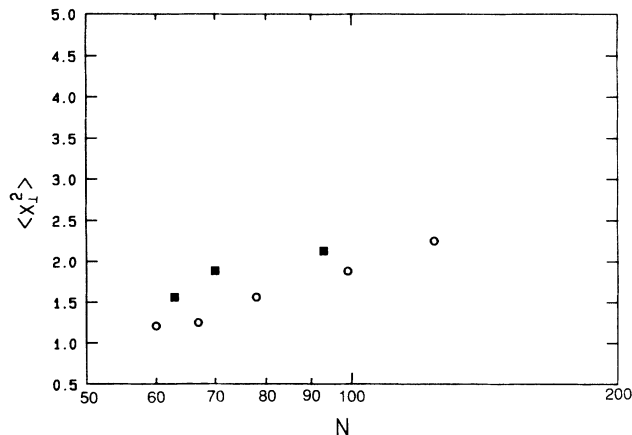


FIG. 4. Phason disorder $\langle X_{\perp}^2 \rangle$ vs number of the ringlike clusters in an annealed $\text{Al}_{65}\text{Cu}_{15}\text{Co}_{20}$. Squares and circles correspond to different samples.

stiffness K deduced from Fig. 4 is 0.1, which is 6 times less than predicted by the random-tiling models.¹⁰⁻¹³

The HREM image of a sample produced by deposition at 400°C [Fig. 2(a)] displays the same ringlike clusters as found in the image of an annealed sample. Moreover, centers of the rings can also be presented in the form of Eq. (1), and the entire micrograph can be covered by the same tiles. There are two major differences between both patterns. First, different tiles in the low-temperature phase are not as uniformly shuffled as in the annealed one. In some regions one can observe sufficiently big clusterings of the similar tiles, or some finite portions of periodic patterns. Such large clusterings of similar tiles are not seen in annealed samples or ideal Penrose tiling. Lifting the coordinate of ring centers to 5D space and projecting them onto perpendicular space confirms this statement quantitatively: $\langle X_{\perp}^2 \rangle$ is found to be approximately 4 times larger than the annealed sample. Moreover, a substantial phason strain has been found. No logarithmiclike behavior in the $\langle X_{\perp}^2 \rangle$ vs N dependence is observed. Second, there are defected regions (tears). These regions are usually curved strips having a width of a couple of ring radii. They cannot be covered by tiles in principle. Nevertheless, the length and, more important, the orientation of the \mathbf{A} vectors are the same on both sides of a tear. When lifted to 5D space, this tiling is represented by a discontinuous surface. The projection of a discontinuity is a tear. Grain boundaries similar to the present tears were found in icosahedral¹⁷ and octagonal¹⁸ phases. As a consequence, an unannealed low-temperature decagonal phase is farther away from the ideal Penrose tiling than an annealed one. This observation supports the suggestion that entropy plays an important role in the quasicrystal formation and stabilization. It is not a direct proof of a random-tiling hypothesis,¹⁰⁻¹³ but it is clear that a thermally activated cluster reshuffling (tile rearrangement) is needed to form a stable quasicrystal. At the least, the decagonal Al-

Cu-Co quasicrystal does not grow according to some growth matching rules.⁶

It is interesting to compare the micrographs of the present stable quasicrystals (both annealed and not annealed) to the images of a metastable Al-Mn decagonal quasicrystal.¹⁹ The latter only has correlation lengths of a few tens of angstroms, even though it has perfect ring-like clusters, similar to those observed in Al₆₅Cu₁₅Co₂₀. The difference between the two patterns is in the distances between the centers of the rings. While in Al₆₅Cu₁₅Co₂₀ all the ring centers are separated exactly by the **A** vectors (except inside tears of unannealed samples), in Al-Mn the spacings and directions of the links vary. There are rings not lying in the sites described by Eq. (1); and there are also unfillable regions. Sometimes it is possible to find finite portions of a tiling even in Al-Mn, but they consist of a few tiles only. The local configurations between such regions resemble tears in Al-Cu-Co.

The authors thank Dr. X. F. Meng for preparing the thin-film samples. S.E.B. is grateful to the University of Virginia for the kind hospitality and to L. S. Levitov and V. Elser for useful discussions. Financial support from U.S. Army Research Office Contract No. DA AL03-87K-0057 is greatly acknowledged.

^(a)On leave from Landau Institute for Theoretical Physics, Moscow, U.S.S.R.

¹L. X. He, Y. K. Wu, and K. H. Kuo, *J. Mater. Sci. Lett.* **7**, 1284 (1987); A. P. Tsai, A. Inoue, and T. Masumoto, *Mater. Trans.* **30**, 300 (1989).

²L. Bendersky, *Phys. Rev. Lett.* **55**, 1461 (1985).

³A. R. Kortan, F. A. Thiel, H. S. Chen, A. P. Tsai, A. Inoue, and T. Masumoto, *Phys. Rev. B* **40**, 9397 (1989).

⁴D. Levine and P. J. Steinhardt, *Phys. Rev. Lett.* **53**, 2477 (1984).

⁵P. A. Kalugin, A. Yu. Kitaev, and L. S. Levitov, *Pis'ma Zh. Eksp. Teor. Fiz.* **41**, 119 (1985) [*JETP Lett.* **41**, 145 (1985)]; *J. Phys. (Paris)* **46**, L601 (1985).

⁶G. Y. Onoda, P. J. Steinhardt, D. P. DiVincenzo, and J. E. S. Socolar, *Phys. Rev. Lett.* **60**, 2653 (1988).

⁷L. S. Levitov, *Commun. Math. Phys.* **119**, 627 (1988); *J. E. S. Socolar, Phys. Rev. B* **39**, 10519 (1989).

⁸S. E. Burkov, *J. Stat. Phys.* **52**, 453 (1988).

⁹R. Penrose, *Bull. Inst. Math. Appl.* **10**, 266 (1974); N. G. de Bruijn, *Nederl. Acad. Wetensch. Proc.* **A84**, 38 (1981).

¹⁰F. Lancon, L. Billard, and P. Chaudhari, *Europhys. Lett.* **2**, 625 (1986); F. Lancon and L. Billard, *J. Phys. (Paris)* **49**, 249 (1988).

¹¹M. Widom, K. Strandburg, and R. H. Swendsen, *Phys. Rev. Lett.* **58**, 706 (1987).

¹²K. Strandburg, L. H. Tang, and M. V. Jaric, *Phys. Rev. Lett.* **63**, 314 (1989).

¹³M. Widom, D. P. Deng, and C. L. Henley, *Phys. Rev. Lett.* **63**, 310 (1989).

¹⁴A. R. Kortan, R. S. Becker, F. A. Thiel, and H. S. Chen, *Phys. Rev. Lett.* **64**, 200 (1990).

¹⁵H. Chen, Y. He, G. J. Shiflet, and S. J. Poon (unpublished).

¹⁶P. A. Kalugin, *Pis'ma Zh. Eksp. Teor. Fiz.* **49**, 406 (1989) [*JETP Lett.* **49**, 467 (1989)].

¹⁷L. A. Bendersky, J. W. Cahn, and D. Gratias, *Philos. Mag.* **B 60**, 837 (1989).

¹⁸N. Wang and K. H. Kuo, *Philos. Mag.* **B 60**, 347 (1989).

¹⁹M. Hirabayashi and K. Hiraga, *Mater. Sci. Forum* **22-24**, 45 (1987).

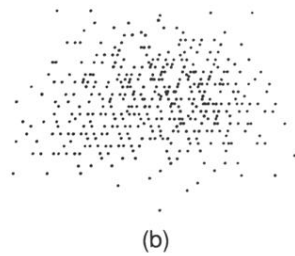
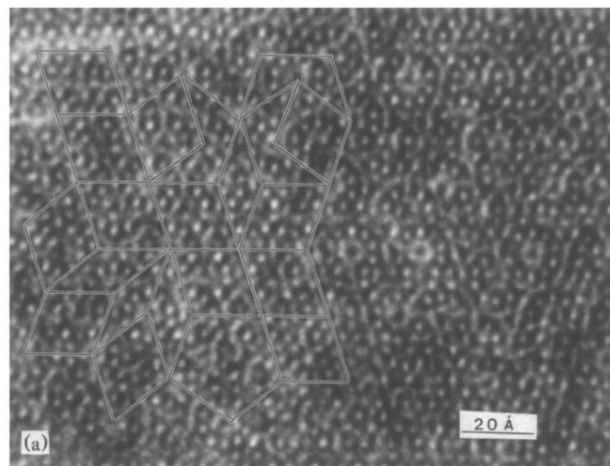
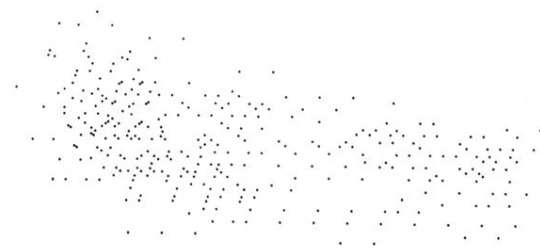
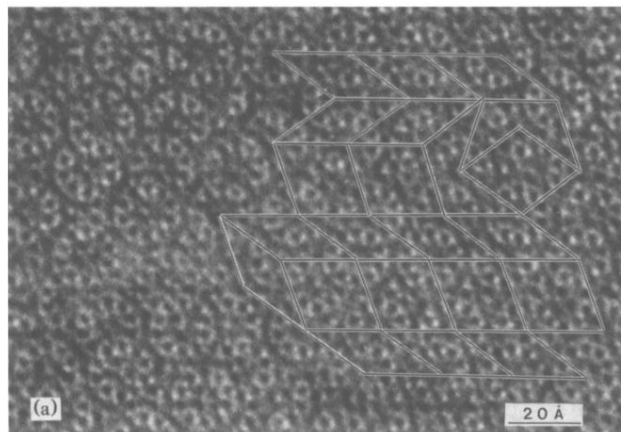


FIG. 1. (a) A portion of HREM image of a decagonal $\text{Al}_{65}\text{Cu}_{15}\text{Co}_{20}$ quasicrystal. The sample was prepared by melt quenching, and was further annealed at 900°C for 24 h. (b) Projection of the ring centers onto the perpendicular space.



(b)

FIG. 2. HREM image of a $\text{Al}_{65}\text{Cu}_{15}\text{Co}_{20}$ sample made by sputter deposition at 400°C , without further annealing. (b) Projection onto the perpendicular space.